Pergamon

SCIENCE DIRECT®

Bioorganic & Medicinal Chemistry Letters 13 (2003) 2527–2530

BIOORGANIC & MEDICINAL CHEMISTRY LETTERS

Synthesis and In Vitro Evaluation of Novel Small Molecule Inhibitors of Bacterial Arylamine *N*-Acetyltransferases (NATs)

Edward W. Brooke,[b] Stephen G. Davies,[a,*] Andrew W. Mulvaney,[a] Minoru Okada,[c] Frédérique Pompeo,[b] Edith Sim,[b] Richard J. Vickers[a] and Isaac M. Westwood[a]

[a]*The Dyson Perrins Laboratory, University of Oxford, South Parks Road, Oxford OX1 3QY, UK*
[b]*Department of Pharmacology, University of Oxford, Mansfield Road, Oxford OX1 3QT, UK*
[c]*Chemistry Laboratories, Institute for Drug Discovery Research, Yamanouchi Pharmaceutical Company Ltd., 21 Miyukigoaka, Tsukuba, Ibaraki, 305-8585, Japan*

Received 10 February 2003; accepted 6 May 2003

Abstract—The synthesis and inhibitory activity of a series of 5-substituted-(1,1-dioxo-2,3-dihydro-1*H*-1λ^6-benzo[*e*][1,2]thiazin-4-ylidene)-thiazolidine-2,4-dione derivatives as competitive inhibitors of recombinant bacterial arylamine-*N*-acetyltransferases (NATs) are described. The most potent NAT inhibitors are those that contain planar hydrophobic substituents on the sultam nitrogen.

Arylamine *N*-acetyltransferases (NATs) encode for a gene family of cytosolic 32-34kDa enzymes which acetylate arylamines, *N*-aryl hydroxylamines[1] and aryl hydrazines[2] using acetyl-CoA as the acetyl donor. NATs are widely distributed in eukaryotes and prokaryotes, with over 20 NATs identified so far in the latter.[3] In Humans one of the two identified NAT isoenzymes, NAT2, inactivates the front-line anti-tubercular drug isoniazid (INH).[4] Interindividual variation in rates of drug metabolism[2,5] and susceptibility to arylamine carcinogens[6] have been linked to polymorphisms in these two Human isoenzymes.[7] Homologues of Human NAT are present in *Mycobacterium tuberculosis* and *Mycobacterium smegmatis* (MSNAT) where they have been shown to acetylate, and hence inactivate, INH.[8] Overexpression of NAT in mycobacteria has been shown to increase their resistance to INH[9] and a *nat* gene knockout of *M. smegmatis* increased sensitivity to the drug.[10] The detection of a NAT polymorphism in drug-resistant isolates of *M. tuberculosis* further suggests that NAT may be involved in INH resistance in tuberculosis.[8] The resurgence of drug-resistance in tuberculosis, especially in relation to the AIDS pandemic, is a major global health problem.[11]

The crystal structure of NAT from *Salmonella typhimurium* (STNAT) has been reported[12] and reveals the protein to consist of three domains such that a cysteine, a histidine and an aspartate residue (Cys^{70}, His^{110}, Asp^{127}; MSNAT nomenclature) are juxtaposed to form a catalytic triad, reminiscent of the cysteine proteases papain and cathepsin.[13] The crystal structure of MSNAT has been resolved to a resolution of 1.7Å and shows a near identical three-dimensional structure to STNAT.[14]

We have instigated a chemical genetics[15] approach to determine the endogenous role of mycobacterial NAT and have identified a novel class of small molecule inhibitors of the pure recombinant enzyme from *M. smegmatis* (MSNAT). High throughput screening of a proprietary small molecule library[16] identified the *N*-(2-naphthyl)-methyl substituted 1,1 - dioxo - 2,3 - dihydrobenzo[1,2]-thiazine-4-ylidene thiazolidine-2,4-dione (TZD-sultam adduct) **1** to be a weak inhibitor of MSNAT-catalysed acetylation of INH, with half-maximal inhibitory concentration (IC_{50}) of 78μM. We report herein the synthesis, in vitro evaluation and preliminary structure–activity relationships (SAR) of a series of TZD-sultam adducts as competitive inhibitors of bacterial NATs.

*Corresponding author: Tel.: +44-1865-275695; fax: +44-1865-275633; e-mail: steve.davies@chem.ox.ac.uk

0960-894X/03/$ - see front matter © 2003 Elsevier Ltd. All rights reserved.
doi:10.1016/S0960-894X(03)00484-0

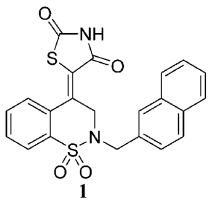

1

Initial structure–activity studies based around **1** revealed that NAT inhibitory activity resided exclusively in compounds incorporating the *N*-substituted TZD-sultam motif; both thiazolidine-2,4-dione (TZD) and **2**, the ketone precursor to **1**, were devoid of NAT inhibitory activity. Similarly, *N*-unsubstituted TZD-sultam adduct **3** was found to be inactive against MSNAT while *N*-alkylation of the TZD moiety in the sultam adducts was also poorly tolerated.[17]

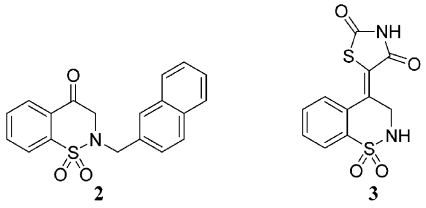

2 3

A series of TZD-sultam adducts was synthesized in which the substituent at the sultam nitrogen atom was systematically varied in order to determine the optimal substituent for binding to MSNAT. Previous studies to determine the substrate specificity of MSNAT revealed lipophilic arylamines to be preferred.[16] Thus a series of lipophilic substituents were introduced at the sultam nitrogen according to Scheme 1.

N-diversification was achieved by alkylation of ketal-protected sultam **4**, with commercially available alkyl and benzylic bromides. Ketal **4** was synthesised in four steps from saccharin.[18] Deketalisation with methanolic hydrogen chloride gave *N*-subsituted ketone **5** which was subsequently condensed with the boron enolate of thiazolidine-2,4-dione to afford the final TZD-sultams **6–18**.[19] The (*E*)-stilbenylmethyl and biphenylmethyl-substituted sultams were synthesized from 4-bromobenzyl intermediate **21**, obtained by alkylation of ketal **4** with 4-bromobenzyl bromide, followed by Heck and Suzuki couplings respectively with styrene and phenylboronic acid. Deprotection and condensation with TZD as before furnished the corresponding TZD-sultams **19** and **20**[20] (Scheme 2).

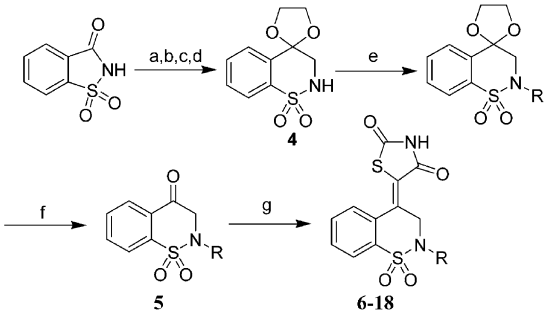

4 5 6-18

Scheme 1. Synthesis of TZD-sultam adducts. Reagents and conditions: (a) NaOH, H_2O, rt, 1 h; (b) $MeCOCH_2Cl$, cetyl trimethylammonium bromide, PhMe, reflux, 12–16 h; (c) NaOEt, EtOH, 55 °C, 0.5 h then HCl(aq), rt, 0.5 h; (d) ethane-1,2-diol, *p*-TsOH, C_6H_6, reflux, 2 h; (e) NaH, DMF rt, 0.5 h then RCH_2Br, rt 12–16 h; (f) HCl, MeOH, THF, reflux, 1 h; (g) thiazolidine-2,4-dione, boron trifluoride diethyl etherate, triethylamine, 1,4-dioxane, 0 °C then rt, 48 h.

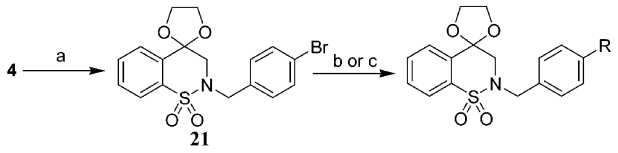

21

Scheme 2. Synthesis of biaryl and stilbenoid derivatives. Reagents and conditions: (a) NaH, DMF rt, 0.5 h then 4-$BrC_6H_4CH_2Br$, rt 12 h; (b) styrene, $Pd(OAc)_2$ (5.0 mol%), P(*o*-tolyl)$_3$ (20.0 mol%), tetra *n*-butyl ammonium bromide, DMF:Et_3N (1:1), 110 °C, 16 h; (c) $PhB(OH)_2$, $Pd(PPh_3)_4$ (5.0 mol%), NaOH, DMF, 100 °C, 32 h.

The *N*-substituted TZD-sultam adducts were evaluated for their in vitro inhibitory activity against recombinant MSNAT-catalysed acetylation of INH by measuring the rate of hydrolysis of acetyl CoA using 5,5′-dithio-bis(2-nitrobenzoic acid),[16,21] with spectrophotometric determination of the product, thio-2-nitrobenzoic acid, λ_{max} 412 nm. The IC_{50} values are summarized in Table 1.

Kinetic analysis of the inhibition was performed by varying the concentration of inhibitor and isoniazid substrate. Inhibition was shown to be competitive with respect to the isoniazid substrate (Fig. 1) and non-linear regression was used to determine the inhibition constant, K_i, for the more potent members of the series (Table 2).

As the crystal structure for MSNAT is now available, in silico docking studies were performed to determine the orientation of binding of the TZD-sultam adducts to the protein. Simulated annealing was achieved using the AutoDock suite of programs as previously described[22] and ten docking solutions were produced for each compound. All the compounds gave exothermic energies of binding that did not necessarily correlate with the level of inhibition observed. However, it was observed that the lowest energy conformations of the most potent

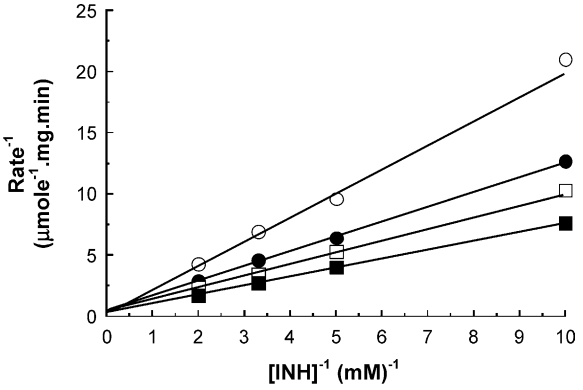

Figure 1. Inhibition of MSNAT by **20**. Double-reciprocal plot of rate against isoniazid concentration in the presence of **20** at 25 μM (open circles), 12.5 μM (filled circles), 6.25 μM (open squares) and 0 μM (filled squares). Non-linear regression (KyPlot) shows the inhibition to be competitive with kinetic parameter $K_i = 14.4$ μM.

Table 1. In vitro inhibition data for inhibition of recombinant MSNAT-catalysed acetylation of INH for selected TZD-sultam NAT inhibitors

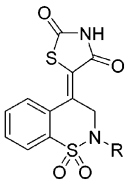

Compd	R substituent	IC_{50} (μM)[a]
1	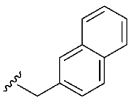	78 ± 5
TZD	—	na
2	—	na[b]
3	H	> 100
6	Me	> 100
7	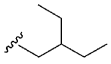	92 ± 5
8	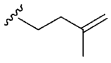	> 100
9	*n*-Octyl	61 ± 8
10	*n*-Decyl	22 ± 2
11		> 100
12		> 100[c]
13	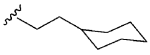	82 ± 10
14	Bn	> 100
15	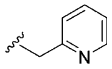	> 100
16	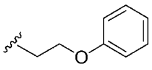	> 100
17	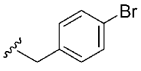	65 ± 5
18	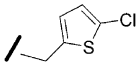	33 ± 1
19	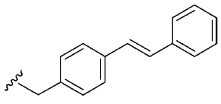	29 ± 2
20	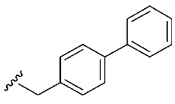	20 ± 1

[a]IC_{50} value were determined from direct regression curve analysis.
[b]na, not active.
[c]IC_{50} = 205 μM.

Table 2. Kinetic parameters for competitive inhibition of MSNAT with respect to isoniazid. Values were determined as in Figure 1

Compd	K_i (μM)
1	70 ± 4
9	43 ± 5
10	14.7 ± 1
18	26.7 ± 2
19	14.0 ± 1
20	14.4 ± 1

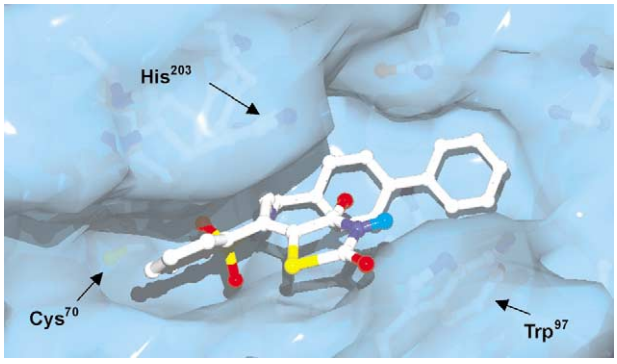

Figure 2. Simulated annealing of **20** to the MSNAT crystal structure. Figure shows the molecular surface of the protein calculated by Swiss PDB Viewer, including the side-chains mentioned in the text, and the lowest energy docking solution of **20** displayed in standard CPK colouring.

inhibitors, listed in Table 2, all showed very similar orientations of binding (shown for **20** in Fig. 2). These docking solutions predict the sultam moiety to be oriented nearest to the active-site cysteine hence blocking binding of the substrate. The variable R group on nitrogen extends into a long groove in the protein, held in place by a tryptophan residue (Trp^{97}). Contact residues around the groove are Phe^{38}, Phe^{130}, Gln^{133}, Val^{169}, His^{203}, Phe^{204}, Asn^{220} and His^{229}. The side-chain of His^{203} appears to be involved in a π-stacking interaction with the thiazolidine-2,4-dione group of the inhibitor, explaining the lack of activity with the ketal and ketone derivatives.

The hydrophobic residues here (Trp, Phe, Val) explain the structure–activity relationship observed, with large hydrophobic (long chain aliphatic and planar aromatic) R-groups on the sultam-TZD adduct providing the greatest inhibition due to non bonding, hydrophobic–hydrophobic and π-stacking interactions between inhibitor and protein. However, there appears to be further potential to improve the potency of this class of NAT inhibitor through targeting of the interactions with the His and Asn residues flanking the active site.

In conclusion we have shown that the TZD-sultam adducts are competitive inhibitors of the acetylation of the anti-tubercular drug isoniazid by mycobacterial NATs. Ongoing work will determine whether these compounds can be used to emulate the phenotype of a genetic knockout in NATs from a range of sources, and whether they affect the sensitivity of the mycobacteria to isoniazid.

Acknowledgements

The authors wish to thank the MRC for a studentship (E.W.B.), the MRC and EPSRC for a Discipline-Hopper Award (R.J.V.), the Blaschko Foundation for a Fellowship (F.P.) and the Wellcome Trust for financial support (E.S.).

References and Notes

1. Hein, D. W.; Doll, M. A.; Rustan, T. D.; Gray, K.; Feng, Y.; Ferguson, R. J.; Grant, D. M. *Carcinogenesis* **1993**, *1*, 1633.
2. Weber, W. W.; Hein, D. W. *Pharmacol. Rev.* **1985**, *37*, 25.
3. Payton, M.; Mushtaq, A.; Yu, T.-W.; Wu, L. J.; Sinclair, J.; Sim, E. *Microbiology* **2001**, *147*, 1137.
4. Evans, D. A. P.; Manley, K. A.; McKuisick, V. A. *Brit. Med. J.* **1960**, *2*, 485.
5. (a) Peters, J. H.; Miller, K. S.; Brown, P. *J. Pharmocol. Exp. Ther.* **1965**, *150*, 298. (b) Jenne, J. W. *J. Clin. Invest.* **1965**, *44*, 1992.
6. Hein, D. W.; Doll, M. A.; Fretland Xiao, G. H.; Devanaboyina, U. S.; Nangju, N. A.; Feng, Y. *Cancer Epidemiology, Biomarkers and Prevention* **2000**, *9*, 29.
7. Upton, A.; Johnson, N.; Sandy, J.; Sim, E. *Trends in Pharmacological Sciences* **2001**, *151*, 846.
8. Upton, A.; Mushtaq, A.; Victor, T. C.; Sampson, S. L.; Sandy, J.; Smith, D. M.; van Helden, P. V.; Sim, E. *Mol. Microbiol.* **2001**, *42*, 309.
9. Payton, M.; Auty, R.; Delgoda, R.; Everitt, M.; Sim, E. *J. Bacteriol.* **1999**, *181*, 1343.
10. Payton, M.; Gifford, C.; Schartau, P.; Hagemeier, C.; Mushtaq, A.; Lucas, S.; Pinter, K.; Sim, E. *Microbiology* **2001**, *147*, 3295.
11. Dye, C.; Scheele, S.; Dolin, P.; Pathania, V.; Raviglione, M. C. *JAMA* **1999**, *282*, 677.
12. Sinclair, J. C.; Sandy, J.; Delgoda, R.; Sim, E.; Noble, M. E. *Nature Structural Biology* **2000**, *7*, 560.
13. Otto, H.-H.; Schrimeister, T. *Chem. Rev.* **1997**, *97*, 133.
14. Sandy, J.; Mushtaq, A.; Kawamura, A.; Sinclair, J.; Sim, E.; Noble, M. E. *J. Mol. Biol.* **2002**, *318*, 1071.
15. (a) Specht, K. M.; Shokat, K. M. *Curr. Opin. in Cell Biol.* **2002**, *14*, 155. (b) Smith, A. *Nat. Rev. Drug Disc.* **2002**, *1*, 95. (c) Stockwell, B. R. *Nat. Rev. Genetics* **2000**, *1*, 116.
16. Brooke, E. W.; Davies, S. G.; Mulvaney, A. W.; Pompeo, F.; Sim, E. *Bioorg. Med. Chem.* **2003**, *11*, 1227.
17. Data not shown.
18. (a) Zinnes, H.; Comes, R. A.; Zuleski, F. R.; Caro, A. N.; Shavel, J., Jr. *J. Org. Chem.* **1965**, *30*, 2241. (b) Zinnes, H.; Comes, R. A.; Shavel, J., Jr. *J. Org. Chem.* **1966**, *31*, 162.
19. All compounds gave satisfactory spectroscopic data. Complete synthetic protocols and spectroscopic data will be reported elsewhere in a full paper.
20. Spectroscopic data for **20**: mp 175–177 °C; IR (KBr) cm^{-1}: 1743 (C=O), 1708 (C=O), 1340 (SO_2^{sym}), 1167 (SO_2^{asym}); ^1H NMR ($CDCl_3$) 400 MHz δ, ppm 4.14 (s, 2H, endocyclic CH_2), 4.95 (s, 2H, $ArCH_2N$), 7.28–8.02 (m, 13H, unresolved Ar); ^{13}C NMR ($CDCl_3$) 100 MHz, δ 52.3, 53.9, 125.2, 127.0, 127.5, 128.2, 128.8, 130.0, 131.1, 131.1, 132.5, 132.7, 133.0, 138.0, 138.6, 140.4, 164.7, 166.1; HRMS (ESI) $(M-H)^-$ $C_{24}H_{17}N_2O_4S_2$ requires 461.0637, observed 461.0630.
21. Riddles, P. W.; Blakeley, R. L.; Zerner, B. *Methods Enzymol.* **1983**, *91*, 49.
22. Mushtaq, A.; Payton, M.; Sim, E. *J. Biol. Chem.* **2002**, *277*, 12175.